SCIENTIFIC REPORTS

OPEN

SUBJECT AREAS:
OTHER NANOTECHNOLOGY
CHEMICAL PHYSICS

Received
2 September 2014

Accepted
31 December 2014

Published
27 January 2015

Correspondence and requests for materials should be addressed to E.S. (strelcove@ornl.gov)

Nanoscale Lubrication of Ionic Surfaces Controlled via a Strong Electric Field

Evgheni Strelcov[1], Rajeev Kumar[1,2], Vera Bocharova[3], Bobby G. Sumpter[1,2], Alexander Tselev[1] & Sergei V. Kalinin[1]

[1]Center for Nanophase Materials Sciences, Oak Ridge National Laboratory, Oak Ridge, TN 37831, [2]Computer Science and Mathematics Division, Oak Ridge National Laboratory, Oak Ridge, TN 37831, [3]Chemical Sciences Division, Oak Ridge National Laboratory, Oak Ridge, TN 37831.

Frictional forces arise whenever objects around us are set in motion. Controlling them in a rational manner means gaining leverage over mechanical energy losses and wear. This paper presents a way of manipulating nanoscale friction by means of in situ lubrication and interfacial electrochemistry. Water lubricant is directionally condensed from the vapor phase at a moving metal-ionic crystal interface by a strong confined electric field, thereby allowing friction to be tuned up or down via an applied bias. The electric potential polarity and ionic solid solubility are shown to strongly influence friction between the atomic force microscope (AFM) tip and salt surface. An increase in friction is associated with the AFM tip digging into the surface, whereas reducing friction does not influence its topography. No current flows during friction variation, which excludes Joule heating and associated electrical energy losses. The demonstrated novel effect can be of significant technological importance for controlling friction in nano- and micro-electromechanical systems.

From synovial joints to digestion in humans, and from gearboxes to microelectromechanical systems in technics, lubrication has proven to be an excellent strategy for controlling frictional forces between the movable parts of a system. A facile way of regulating the sliding friction in water-based lubricants via electrochemistry was discovered by Thomas A. Edison in 1874[1]. In the following century the mechanisms behind the bias dependence of friction in electrolytes were extensively investigated both at the macro[2,3] and nanoscale[4–9]. It has been proposed that the friction coefficient may change in response to adsorption of species, their re-orientation in the electric field, surface oxidation or reduction, deposition of monolayer films and accumulation of alkali or acidic products at the moving electrode. Despite these efforts, only an increase in the friction force at the onset of electrochemical reactions has been demonstrated for nanosystems, and the concomitantly flowing currents lead to electric power losses. In addition, application of a liquid lubricant necessitates existence of a bulky and liquid-tight reservoir as well as a sprinkling mechanism. It is clearly desirable to avoid these complications in micro- and nanomechanical devices, while still having control over friction.

Water has been used as a lubricant since the dawn of civilization[10]. It is also naturally present in ambient air and, therefore, can be condensed from it onto a surface of interest for lubrication. A straightforward method of water vapor liquefaction is cooling. However, it implies large energy consumption, low switching speed due to thermal flow impediments and non-local water coverage. A better solution is to replace thermal energy with another thermodynamic force such as a strong confined electric field, to assure vapor condensation[11] in only pre-defined locations. Here we report a novel physical effect that allows tuning nanoscale friction on ionic surfaces via electric field-controlled condensation of lubricant at the moving joint from the ambient gas phase. This finding can have a significant technological impact allowing decreasing or increasing nanoscale friction at will and thus controlling energy losses and wear of micro-electromechanical systems (MEMS) parts.

Results

We have used ambient probe atomic force microscopy (AFM) to measure nanoscale friction as a function of the voltage applied to the conductive AFM tip and air humidity. The difference between the lateral deflection during the forward and reverse scans was used as a measure of the sliding friction coefficient between the tip and surface[9,12,13]. Various metal salts and several molecular solids were investigated. Figures 1 A and B show that at 45% relative air humidity (RH) application of up to ± 7 V to the AFM tip does not change the friction coefficient on a magnesium sulfate surface in any appreciable way. Increasing the humidity level up to 60% also

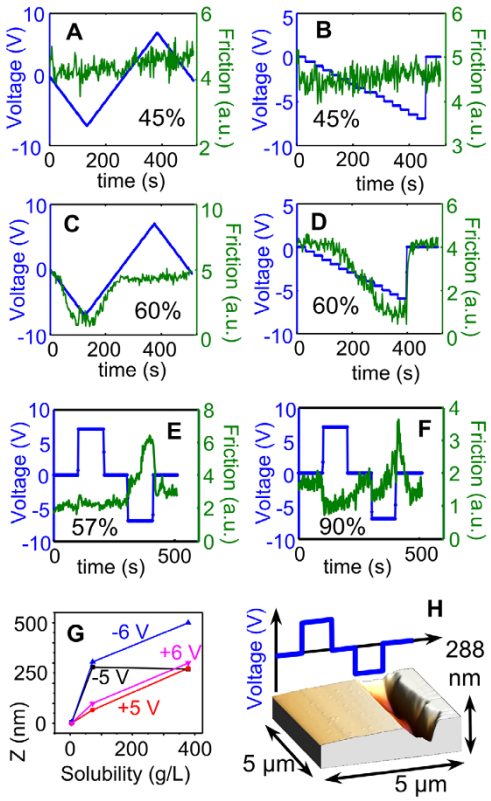

Figure 1 | Tuning friction with bias and humidity. (A–D) Friction and tip bias as a function of time for (A–B) $MgSO_4 \cdot 7H_2O$ at 45% relative humidity: no change in friction for both bias polarities; (C–D) $MgSO_4 \cdot 7H_2O$ at 60% relative humidity: friction decreases drastically below −2.5 V, but doesn't change at positive bias; (E) KIO_4 at 57% relative humidity: friction increases at negative bias; (F) KIO_4 at 90% relative humidity: friction initially decreases upon application of both positive and negative bias, but later on increases in response to a constant negative bias; (G) Tip penetration depth as a function of salt (KIO_4, KNO_3, alum) solubility in water (in the absence of an electric field) for several tip biases; (H) topographic image of KIO_4 surface recorded simultaneously with the data shown in panel F: negative bias damages the surface, which brings about an increase in friction.

does not lead to any notable influence on friction. It takes a combination of a higher humidity and applied bias to reduce friction by about 5-fold (Fig. 1 C & D). Sweeping the DC bias slowly or changing it stepwise reveals that the underlying process starts below a threshold bias of −2–2.5 V and the friction force returns to its initial value after the electric field is switched off (within 2–3 scanning lines or 4–6 s). Interestingly, this effect is polarity-dependent; at a positive bias, friction remains at its original high level (Fig. 1C). Other salts show similar behavior, manifesting the existence of both humidity and bias thresholds, past which the friction force starts to deviate from its initial value. For instance, a potassium periodate surface is not responsive to +7 V bias at 57% RH (Fig. 1E), whereas at 90% RH, the same bias brings about an approximately two-fold decrease in friction (Fig. 1F). On the other hand, negative bias (−7 V) at 57% RH increases friction force 3-fold and at 90% RH first reduces and then raises it. Thus, different from the previous reports, the observed effect allows manipulation of the friction coefficient in both directions paving the way for a rational control over nanoscale friction. It is noteworthy that the increase in friction force is associated with significant topographic changes, as the AFM tip burrows a trench into the material during surface scanning (Fig. 1H). On the contrary, in the diminished friction regime, the surface topography remains unchanged.

In order to explore this effect further we conducted similar experiments on surfaces of molecular rather than ionic solids, with vastly different water solubility: sucrose, urea (both highly soluble), polystyrene and quartz (both insoluble). None of these substances manifested any variation of friction in the humidity range from 0 to 92% and at tip biases ±90 V (see Suppl. Mat. Fig. S1). This fact, as well as a non-trivial polarity dependence, hints at an electrochemical rather than a pure physical mechanism for the bias-dependent friction effect, which calls for current measurements. Hence, to explore the origins of this behavior we utilized the AFM technique of first order reversal curve current-voltage-topography (FORC-IVz) spectroscopy[14] to understand how current and vertical tip position vary during bias sweeps from zero to a maximal value and back, as the tip is parked at one location (Fig. 2A). A typical FORC-IVz triangular voltage waveform is shown in Figure 2F. All of the subsequent experiments were performed on alkali and alkali-earth metal salts. It follows that a detectable current appears only at RH higher than 75% and quickly vanishes after measurements at several locations are performed (Fig. 2G). Rinsing the AFM tip in deionized water helps in restoring the current, but only for a few additional measurement locations (see Supl. Mat. Fig. S2). Apparently the salt solution crystallizes on the cantilever tip forming an insulating layer that prevents current from flowing. Experiments on samples mounted on an insulating substrate without a bottom electrode and no current sink have shown that bias-controlled friction tuning is possible without any current flow. However, as the biased tip scans the surface, it slowly becomes charged, which screens the electric field of the tip and eventually leads to loss of control over friction. Minuscule surface charge scavenging restores the control without measurable current flows. We point out that absence of current is highly beneficial from a power-saving prospective, as it eliminates Joule heating and other parasitic power-consuming effects.

Howbeit, the vertical position of the cantilever varies more predictably and is independent of the current, with the tip plunging deep into the crystal as the tip bias or RH are increased above the threshold values. For instance, Figure 2F shows how the tip's vertical position varies over time as a bias waveform is applied to the cantilever. As can be seen, nothing happens during the first triangular voltage pulse with the peak bias of −1 V, but on the second and third pulses, when bias is swept below −1.5 V, the tip starts plunging into the sample. It is this penetration that leads to an increase in friction and changes in surface topography as was discussed above, thus it is a measure of increase in friction. The plunge depth is proportional to the peak bias and solubility of the salt (Fig. 1G). More systematically, Figure 3 presents a phase diagram of the tip plunge depth for one of the studied salts, alum ($KAl(SO_4)_2 \cdot 12H_2O$). The humidity and tip bias act as slightly interdependent driving forces of the process. That is, at very low humidity no voltage is adequate to initiate tip descent, and at zero bias and RH higher than 85% it leads to only a slow drift of the tip into the material, not a sharp plunge (see Suppl. Mat. Fig. S1 C&F). In other regions of the phase diagram the tip can be brought into descent by increasing either RH or bias. We note again a clear asymmetry of the bias polarity influence. Like the $MgSO_4$ and KIO_4 cases, for the alum crystal negative bias has a greater effect on the tip displacement than the positive bias. At RH higher than 65–70% and voltages more than 3 V the tip plunge becomes enormous (up to 1.5 μm), and is very unstable and poorly reproducible (therefore, these data are excluded from the phase diagram of Fig. 3). An example of surface patterning after a FORC-IVz measurement on a 3 × 3 grid is shown in the inset of Figure 3.

Discussion

In considering the possible mechanisms of the observed effects one should account for the following: (1). Any friction change/tip penetration requires simultaneous fulfilment of 3 conditions: a) RH above a threshold value, b) voltage above a threshold value, c) ionic

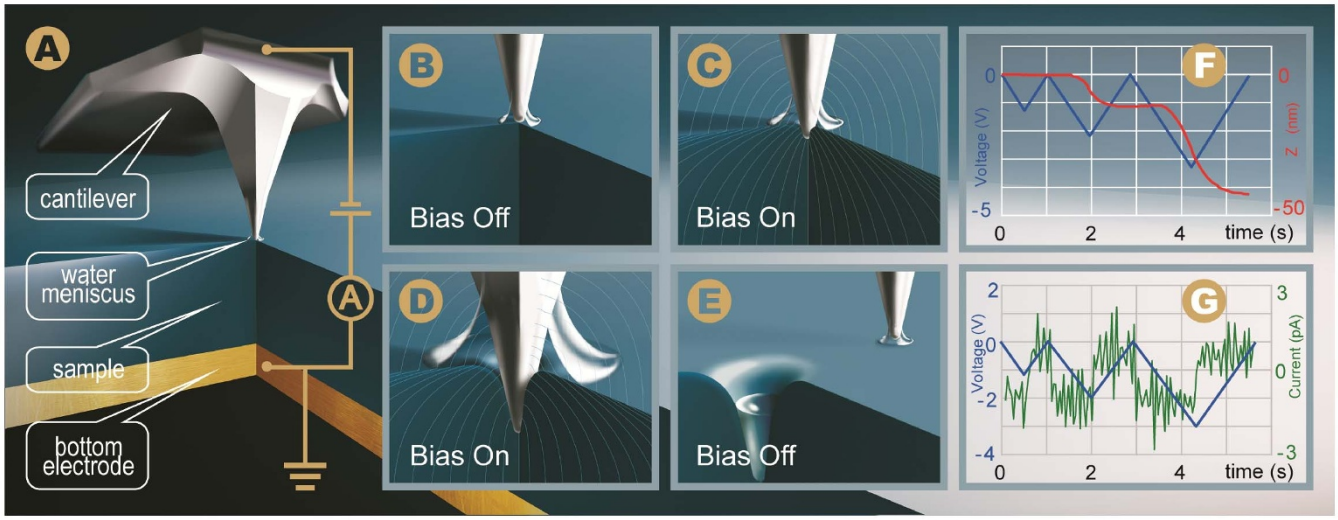

Figure 2 | FORC-IVz measurements. (A) Measurements schematics: as an AFM tip with a conductive coating is parked at one sample location, a DC bias waveform is applied to it and a current is read from the bottom electrode. A water meniscus is formed at the tip-surface junction at high humidity due to its negative curvature. (B–E) A cartoon representation of the observed process in the vicinity of the tip-surface junction. (B) The starting position with bias off and a small meniscus; (C) The electric field is switched on, the meniscus increased and the tip started plunging into the sample; (D) After some time the tip has penetrated deep into the sample; (E) The electric field is switched off, the tip was moved to a new location for the next measurement leaving a hole behind; (F) Measured tip position and the bias waveform plotted vs. time (alum, 40% RH); (G) No steady current is detected, only capacitive jumps are seen at the voltage waveform turning points.

material surface; (2). The RH threshold value for different salts varies significantly (from 30 to 90%) and is inversely proportional to the salt solubility; (3). The bias threshold value varies little (1.5–6 V) and is somewhat dependent on the RH; (4). Friction change/tip penetration is independent of current and in most cases no current flows; (5). Friction change/tip penetration strongly depends on bias polarity but can be opposite for different salts.

Understanding the observed phenomena is complicated by their nanoscale nature and the extreme conditions at the tip-surface junction, where pressure can reach the GPa range and the confined electric field can be on the order of 10^7–10^8 V/m. A plethora of unusual effects can manifest themselves in materials behavior in such strong electric fields, including water freezing[15,16], ice melting[17–20], water vapor condensation[11,21], gigantic electrostriction[22], etc. In addition, electrochemically-controlled nano/microscale dissolution of inorganic salts has been demonstrated for low electric fields and in saturated solutions[23–25]. However, based on our observations, most of these effects can be excluded as possible explanations. Independence of the friction/tip penetration of the current rules out electrochemical dissolution, as it is driven by the undersaturation created by electrochemical conversion of one of the ions constituting the salt. In addition, many of the salts we have tested are comprised of ions that do not undergo any electrochemical reactions in aqueous solutions for the studied potential range (e.g. K^+, Na^+, NO_3^-, SO_4^{2-}, etc.). Water splitting with formation of acidic/alkali solution at the tip-surface junction is also impossible without appreciable current, and is unlikely to have a major contribution. Likewise, the absence of current eliminates Joule heating and related thermal degradation of the materials. Pressure alone is also unlikely to be the driving force, as in the absence of bias or in a dry atmosphere the tip is stable and does not penetrate the ionic crystals. Friction can be linked to an increase in surface wettability induced by charge injection from the biased tip. However, the studied surfaces have extremely high water affinity per se, and their wettability can hardly be changed without drastically affecting their chemical composition. Hence, contribution of this mechanism to the observed effect should be minimal. It is known that water vapors condense at the AFM tip-surface junction at ambient humidity or higher[26]. In a strong electric field condensation is enhanced due to a gain in energy achieved by reducing the electric field strength by a factor of the water dielectric constant[11]. It could be imagined that water condensation could lubricate the junction, decrease the friction and even dissolve some of the sample beneath the tip, thereby leading to its plunge. This simple condensation-dissolution mechanism, however, is independent of the type of the surface used for condensation, which contradicts our observations. Despite the fact that both urea and sucrose are much more soluble than the salts used in our studies, they are insensitive to the applied bias, and probably only the phenomenon of slow downward drift of the tip into them at high humidity can be explained with this condensation-dissolution hypothesis (see Suppl. Mat. Fig. S1).

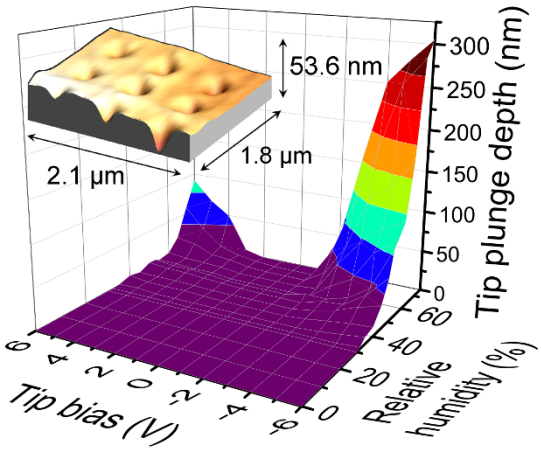

Figure 3 | Tip bias-humidity phase diagram for alum. Average tip penetration depth (proportional to friction increase) as a function of peak tip bias for a one triangular pulse DC voltage waveform and ambient relative humidity. The inset shows a topographic image of the alum surface after performing 9 FORC-IVz measurements over a 3 × 3 grid of spatial locations at 35% RH. The depth of the holes formed is in the range of 12–40 nm and a width of about 250 nm. Note that this is much larger than the size of the tip.

Having considered all of the above scenarios that were found highly improbable based on our experiments, we propose the follow-

ing plausible mechanism of the observed effects. The water condensed at the tip-surface junction in the absence of an electric field forms a saturated solution droplet on any kind of soluble crystal. However, behavior of this droplet in a strong electric field, would depend on whether it is strongly polarizable (contains movable ions) or not (contains non-charged molecules). In the former case, the system will try to minimize its free energy by adsorbing ions on the tip surface (electrode) and forming an electric double layer (EDL). The ordered structure of the EDL can be responsible for a decrease in the friction coefficient between the tip and surface[27]. Solutions of molecular solids will form a very weak double layer consisting of polarized water molecules, thus leaving friction unchanged. The structure of the EDL will depend on the nature of ions, especially, on their charge and size. This can explain the strong voltage polarity dependence for the friction lowering effect. Existence of RH and bias thresholds as well as their dependence on salt solubility follows naturally from this model. Water condensation in a strong electric field plummets above a certain field strength (see Fig. 2 in Ref. 11), and the amount of ions capable of forming a EDL is directly proportional to the salt solubility. Importantly, the formation of an EDL (in contrast to electrochemical reactions) is associated with a small capacitive current that could be undetectable in our experimental setup. Finally, dissolution of salts in water significantly decreases its dielectric constant, whereas minimization of free energy in a strong electric field requires it to increase. Thus, there exists a thermodynamic force that should expel a salty solution from the vicinity of the tip-surface junction outward, spreading it along the surface and replacing it with a fresh water (with higher dielectric constant) condensed from the vapor. Alternatively, an electrostatic instability in a charged droplet can cause its micro-explosion with the same effect: brine is ousted from the tip vicinity. The expelled solution will carry away dissolved salt from beneath the tip, forcing it to start a downward motion. This process should continue while the electric field is on, and nothing prevents water from being condensed, solution from being spread outward (or upward along the tip surface), and the tip from moving. It should be noted that aqueous solutions of molecular solids also have a lower dielectric constant than pure water, which means that the mechanism behind the tip plunge is more complicated than what is described here and further experiments/modeling is required to fully unravel it.

Methods

Measurements were performed on a Multimode 8 AFM platform (Bruker) equipped with a Nanonis controller and a gas cell. The bias application and signal recording was done by a computer via a National Instruments card controlled through the MatLab/LabView software. A current amplifier (Femto DLPCA-200) was used for current detection. AFM tips (Budget Sensors, k = 3 N/m) with conductive Cr/Pt coating were used. FORC-IVz measurements were performed on 3 × 3 grids of spatial locations with separations chosen each time in such a way that the adjacent measurement did not influence each other. At low humidity levels, when the hole formed by the tip is small, a 1 × 1 μm^2 region was sufficient. At very high humidity levels, 10 × 10 μm^2 regions were used for same grid size. All of the presented figures show cantilever vertical positions and current data averaged over the 9 points of the grid. The voltage waveform consisted of one triangular DC bias pulse (except data shown in Fig. 2 and Fig. S2). The following chemicals were investigated: sodium thiosulfate, sodium acetate, sodium chloride, sodium nitrate, magnesium sulfate, potassium nitrate, alum, potassium periodate, potassium chloride, glass, quartz, sucrose, urea, and polystyrene. Millimeter-size crystals of water-soluble salts were grown from aqueous solutions and glued with silver paint onto a copper circuit board that served as a current collector. For samples on insulating substrates without the bottom electrode, quartz slides were used. Crystals were grown when the indoor ambient RH was ca. 40–45%. A polystyrene film (several μm thick) was prepared by drop-casting a polystyrene solution (in benzene) onto a silicon wafer with a pre-deposited gold electrode. Data processing was done using custom-written Matlab codes.

1. Edison, T. A. Improvement in Telegraph Apparatus. *United States patent* 158,787. 1875 Jan 19.
2. Clark, R. E. D. The influence of electric potentials upon friction. Part I.-In aqueous solutions of salts. *Trans. Faraday Soc.* **42**, 449–456, DOI:10.1039/tf9464200449 (1946).
3. Dubois, J. E., Lacaze, P. C., Courtel, R., Herrmann, C. C. & Maugis, D. Polaromicrotribometry: A Friction Method for the Study of Polarized Metal Solution Interfaces: Application to the Gold Electrode. *J. Electrochem. Soc.* **122**, 1454–1460, DOI:10.1149/1.2134041 (1975).
4. Campbell, S. D. & Hillier, A. C. Nanometer-Scale Probing of Potential-Dependent Electrostatic Forces, Adhesion, and Interfacial Friction at the Electrode/Electrolyte Interface. *Langmuir* **15**, 891–899, DOI:10.1021/la981137u (1999).
5. Nielinger, M. & Baltruschat, H. Nanotribology under electrochemical conditions: influence of a copper (sub)monolayer deposited on single crystal electrodes on friction forces studied with atomic force microscopy. *Phys. Chem. Chem. Phys.* **9**, 3965–3969, DOI:10.1039/b706804b (2007).
6. Sweeney, J. *et al.* Control of Nanoscale Friction on Gold in an Ionic Liquid by a Potential-Dependent Ionic Lubricant Layer. *Phys. Rev. Lett.* **109**, 155502–155504 (2012).
7. Labuda, A. *et al.* Switching Atomic Friction by Electrochemical Oxidation. *Langmuir* **27**, 2561–2566, DOI:10.1021/la104497t (2011).
8. Hausen, F., Nielinger, M., Ernst, S. & Baltruschat, H. Nanotribology at single crystal electrodes: Influence of ionic adsorbates on friction forces studied with AFM. *Electrochim. Acta* **53**, 6058–6063, DOI:10.1016/j.electacta.2008.03.053 (2008).
9. Carpick, R. W. & Salmeron, M. Scratching the surface: Fundamental investigations of tribology with atomic force microscopy. *Chem. Rev.* **97**, 1163–1194, DOI:10.1021/cr960068q (1997).
10. Fall, A. *et al.* Sliding Friction on Wet and Dry Sand. *Phys. Rev. Lett.* **112**, 175502–175505 (2014).
11. Butt, H.-J., Untch, M. B., Golriz, A., Pihan, S. A. & Berger, R. Electric-field-induced condensation: An extension of the Kelvin equation. *Phys. Rev. E* **83**, 061604–061605 (2011).
12. Varenberg, M., Etsion, I. & Halperin, G. An improved wedge calibration method for lateral force in atomic force microscopy. *Rev. Sci. Instrum.* **74**, 3362–3367, DOI:10.1063/1.1584082 (2003).
13. Ogletree, D. F., Carpick, R. W. & Salmeron, M. Calibration of frictional forces in atomic force microscopy. *Rev. Sci. Instrum.* **67**, 3298–3306, DOI:10.1063/1.1147411 (1996).
14. Strelcov, E. *et al.* Probing Local Ionic Dynamics in Functional Oxides at the Nanoscale. *Nano Letters* **13**, 3455–3462, DOI:10.1021/nl400780d (2013).
15. Jinesh, K. B. & Frenken, J. W. M. Experimental Evidence for Ice Formation at Room Temperature. *Phys. Rev. Lett.* **101**, 036101-036101-036101-036104 (2008).
16. Ehre, D., Lavert, E., Lahav, M. & Lubomirsky, I. Water Freezes Differently on Positively and Negatively Charged Surfaces of Pyroelectric Materials. *Science* **327**, 672–675, DOI:10.1126/science.1178085 (2010).
17. Danielewicz-Ferchmin, I., Banachowicz, E. & Ferchmin, A. R. Water phases under high electric field and pressure applied simultaneously. *J. Mol. Liq.* **135**, 75–85, DOI:10.1016/j.molliq.2006.10.006 (2007).
18. Shevkunov, S. V. Melting of Water Molecule Clusters in a Strong Electric Field under the Conditions Modeling Arctic Stratosphere. *Colloid J.* **63**, 511–517, DOI:10.1023/a,1016774409809 (2001).
19. Danielewicz-Ferchmin, I. & Ferchmin, A. R. Lowering of the freezing temperature of water at the protein surface due to electric field. *J. Mol. Liq.* **124**, 114–120, DOI:10.1016/j.molliq.2005.09.004 (2006).
20. Qiu, H. & Guo, W. L. Electromelting of Confined Monolayer Ice. *Phys. Rev. Lett.* **110**, 195701–195704, DOI:10.1103/PhysRevLett.110.195701 (2013).
21. Maerzke, K. A. & Siepmann, J. I. Effects of an Applied Electric Field on the Vapor-Liquid Equilibria of Water, Methanol, and Dimethyl Ether. *J. Phys. Chem. B* **114**, 4261–4270, DOI:10.1021/jp9101477 (2010).
22. Danielewicz-Ferchmin, I. & Ferchmin, A. R. A critical point related to phase transitions in electrostricted H_2O close to an electrode. *Chem. Phys. Lett.* **398**, 186–189, DOI:10.1016/j.cplett.2004.09.051 (2004).
23. Macpherson, J. V. & Unwin, P. R. Oscillatory Dissolution of an Ionic Single Crystal Surface Observed with the Scanning Electrochemical Microscope. *J. Phys. Chem.* **98**, 11764–11770, DOI:10.1021/j100096a022 (1994).
24. Macpherson, J. V. & Unwin, P. R. Scanning Electrochemical Microscopy as a Probe of Silver Chloride Dissolution Kinetics in Aqueous Solutions. *J. Phys. Chem.* **99**, 14824–14831, DOI:10.1021/j100040a037 (1995).
25. Macpherson, J. V. & Unwin, P. R. Scanning Electrochemical Microscope Induced Dissolution: Rate Law and Reaction Rate Imaging for Dissolution of the (010) Face of Potassium Ferrocyanide Trihydrate in Nonstoichiometric Aqueous Solutions of the Lattice Ions. *J. Phys. Chem.* **99**, 3338–3351, DOI:10.1021/j100010a052 (1995).
26. Weeks, B. L., Vaughn, M. W. & DeYoreo, J. J. Direct Imaging of Meniscus Formation in Atomic Force Microscopy Using Environmental Scanning Electron Microscopy. *Langmuir* **21**, 8096–8098, DOI:10.1021/la0512087 (2005).
27. de Wijn, A. S., Fasolino, A., Filippov, A. E. & Urbakh, M. Nanoscopic Friction under Electrochemical Control. *Phys. Rev. Lett.* **112**, 055502–055505 (2014).

Acknowledgments

This research was conducted at the Center for Nanophase Materials Sciences, which is sponsored at Oak Ridge National Laboratory by the Scientific User Facilities Division, Office of Basic Energy Sciences, U.S. Department of Energy. VB would like to acknowledge sponsorship by the Laboratory Directed Research and Development Program of Oak Ridge

National Laboratory, managed by UT-Battelle, LLC, for the U. S. Department of Energy. ES and SVK would like to thank Dr. P. Collier for fruitful discussion. ES gratefully acknowledges Mr. A. Strelkov for his help in illustrating this manuscript.

Author contributions

E.S. designed and performed the experiment, and wrote the manuscript, S.V.K. designed the experiment and guided research; E.S., R.K., V.B., B.G.S., A.T. and S.V.K. participated in data interpretation, discussion and manuscript review.

Additional information

Supplementary information accompanies this paper at http://www.nature.com/scientificreports

Competing financial interests: The authors declare no competing financial interests.

How to cite this article: Strelcov, E. *et al.* Nanoscale Lubrication of Ionic Surfaces Controlled via Strong Electric Field. *Sci. Rep.* **5**, 8049; DOI:10.1038/srep08049 (2015).